Program Digest, 2019 IEEE International Ultrasonics Symposium (IUS)
Glasgow, Scotland, October 6-9, 2019

Design of Wide-Band Asymmetric Hybrid Ladder Filters

Michael Wagner
Intel Deutschland GmbH
Neubiberg, Germany
michael1.wagner@intel.com

Timo Gossmann, Jakob Tomasik
Intel Deutschland GmbH
Neubiberg, Germany

Robert Weigel
Institute for Electronics Engineering
University of Erlangen-Nuremberg
Erlangen, Germany

Amelie Hagelauer
Chair of Communications Electronics
University of Bayreuth
Bayreuth, Germany

Abstract—**In this paper, a new type of hybrid ladder filter is presented to be used in asymmetric wide-band filter designs. The concept is based on simple filter stages that may be cascaded in a ladder-type topology. The single filter stages each employ acoustic-wave resonators and other lumped elements in certain combinations that allow for steep filter skirts on one side of the passband and theoretically unlimited bandwidth. An algorithm for the design of arbitrarily-wide-band filters with fixed properties of acoustic-wave resonators is given. Furthermore, simulation and measurement results of a prototype filter stage are presented, that prove the concept to be feasible.**

I. Introduction

Modern communication systems make high demands on the employed filters and duplexers used in RF front-ends [1]. For wireless communication standards up to 6 GHz, acoustic-wave resonators (AWRs) are the dominating technology for filter purposes. They make use of the piezoelectric effect and their operation therefore depends on the properties of the used materials [2]. One characteristic constant of any acoustic-wave resonator is its effective electro-mechanical coupling coefficient (EMCC) k_{eff}^2.

A great advantage of acoustic-wave resonators in general is their very high quality factor: Q factors greater than 1000 are state of the art [3]. They also have high power handling capability and require only small area [4]. However, filters made of AWRs have limited fractional bandwidth (FBW), that depends on the EMCC [3]. For the realization of wide-band filters of high quality, much research has been conducted to make use of new materials with improved properties [5].

On the other hand, there is classical filter theory that is using inductors and capacitors for the realization of mathematically described filter transfer functions. Their limit in realizability mostly depends on the component values and the physical size of the elements. Theoretically, pure LC filters are unlimited in bandwidth, but their elements exhibit only poor quality (especially inductors), much lower than it is possible with AWRs [4].

This paper presents a hybrid filter approach, combining some of the respective benefits of acoustic-wave and LC resonators. Two complementary simple stages for hybrid ladder filter design are shown, that can easily be cascaded to form a ladder-type filter topology with beneficial characteristics. The design process is described and measurements for one type of single stage are shown.

II. Acoustic-Wave Resonators and Filters

An acoustic-wave resonator is an electromechanical component that uses a piezoelectric material layer for the transformation between electrical and mechanical (acoustic) waves. Depending on the acoustic wave mode, different types of AWRs have evolved. SAW resonators make use of surface acoustic waves, whereas BAW resonators depend on bulk acoustic waves [6], [7].

AWRs are typically described by the modified Butterworth-van-Dyke (BVD) model [8]. It is shown for an ideal (lossless) resonator in Fig. 1. The BVD model is an equivalent circuit that describes the electrical behavior of the AWR at its terminals.

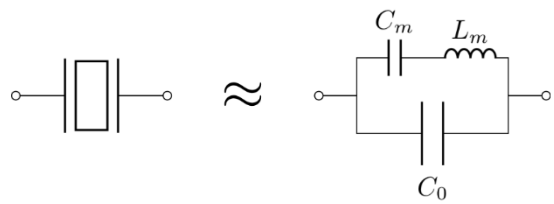

Fig. 1. Lossless BVD model of an acoustic-wave resonator

The resonator's behavior at the electrical terminals is dominated by its static capacitance C_0. A series resonance (f_r) is created by the reactive elements of the motional branch (L_m, C_m), and the parallel combination with the static capacitance leads to a parallel resonance, or anti-resonance (f_{ar}), at a higher frequency than the series resonance. The distance between these two resonance frequencies is an important characteristic of the resonator. When used in filter designs, the achievable bandwidth is limited by this distance. It depends on resonator architecture and properties of the employed materials.

The resonance and anti-resonance frequency are related to the elements of the equivalent circuit model by:

$$\omega_r = 2\pi f_r = \frac{1}{\sqrt{L_m C_m}} \tag{1}$$

$$\omega_{ar} = 2\pi f_{ar} = \frac{1}{\sqrt{L_m \frac{C_m C_0}{C_m + C_0}}} = \omega_r \cdot \sqrt{1 + \frac{1}{r}} \tag{2}$$

where r is defined as the capacitance ratio:

$$r := \frac{C_0}{C_m} \tag{3}$$

The effective electro-mechanical coupling coefficient depends on the resonant frequencies. This relationship is given by [9]:

$$k_{\text{eff}}^2 = \frac{\pi^2}{4}\frac{f_r}{f_{ar}}\frac{f_{ar}-f_r}{f_{ar}} \approx \frac{\pi^2}{4}\frac{f_{ar}-f_r}{f_{ar}} \tag{4}$$

It can also be expressed as a function of r by [8]:

$$k_{\text{eff}}^2 = \frac{\pi^2}{8}\frac{1}{r}\left(1-\frac{1}{r}\right) \tag{5}$$

The element values of an AWR depend on the resonator type, targeted operation frequency, physical size and employed materials.

For filter applications, AWRs are typically combined in ladder-type structures. An example with 5 elements is shown in Fig. 2a. The series and shunt resonators exhibit different resonances so that the series resonance of the series elements coincides with the anti-resonance of the shunt elements. Therefore, in the designated passband the series resonators are highly conductive whereas the shunt resonators have high impedance. Notches on the lower and upper side of the passband are caused by the series resonance of the shunt elements (creating a short to ground) and the anti-resonance of the series elements (creating an open in the forward path), respectively. The operation principle is depicted in Fig. 2b, including the resonator admittance of some example resonators and the corresponding filter transfer function.

The typical fractional bandwidth (FBW) for a ladder-type filter is limited by the EMCC of the single resonators. It is in the order of 0.4 k_{eff}^2 [5].

III. Hybrid Ladder Filter Design

In this section the new concept is presented that can be used for hybrid ladder filter design.

A. Single Filter Stages

There are two complementary filter stages on which the following examination is based. They are depicted in Fig. 3.

One stage consists of an AWR in the series branch, while comprising two shunt branches with equal parallel LC resonators (pLCR), forming a π-type structure. The other stage has an AWR in the shunt branch and a series LC resonators (sLCR) in each of its series branches, forming a T-type structure. The important characteristic is, that a single AWR is used only in either series or shunt branch. The filter response of the π-section with series AWR exhibits a notch ($f_{2\infty}$) in the upper stopband. It is therefore used for filters that require a sharp roll-off near the upper passband edge (f_2). The T-section causes a notch ($f_{1\infty}$) in the lower stopband and can be used for filters with sharp roll-off near the lower passband edge (f_1). The behavior of the single stages is illustrated in Fig. 3c for an example AWR with a series resonance at 1.7 GHz.

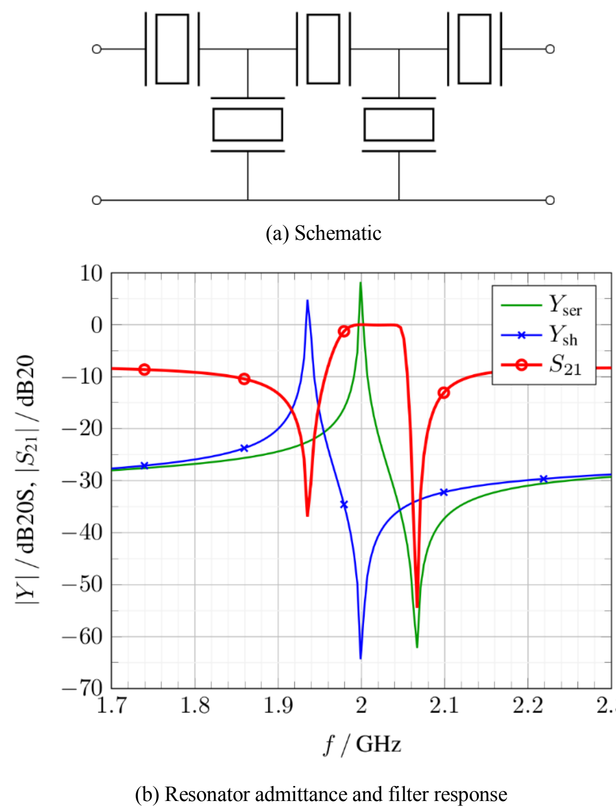

Fig. 2. Working principle of a ladder-type acoustic-wave filter, example structure consisting of 5 resonators

When using the lossless BVD model for the AWRs, design equations developed by Zobel [10] can be used for the single stages. They are not repeated here. It must be noted that in this case the variables f_1 and f_2 do not represent the 3 dB corner frequency. Nevertheless, they give a good approximation for the estimation thereof.

For the application of Zobel's design equations, three frequencies must be known: the corner frequencies of the desired passband (f_1, f_2) and the notch frequency caused by the resonator ($f_{1\infty}$ or $f_{2\infty}$). This is the series or anti-resonance of the resonator for T- or π-structure, respectively. Typically, the notch frequency and bandwidth of the filter are specified, i.e. the corner frequency on the other passband edge of the resonator is defined. The corner frequency that is closer to the resonator depends on the capacitance ratio of the resonator (or k_{eff}^2, resp.) and can be calculated by the following equations.

For the pi section ($f_1$and $f_{2\infty}$ are defined):

$$f_2 = \frac{f_{2\infty}}{\sqrt{1+\frac{1}{(q^2-1)\,r^2}}}, \qquad \text{with } q = \frac{f_{2\infty}}{f_1} \tag{6}$$

For the T section ($f_{1\infty}$ and f_2 are defined):

$$f_1 = f_{1\infty}\cdot\sqrt{1+\frac{1}{(q^2-1)\,r^2}}\,, \qquad \text{with } q = \frac{f_2}{f_{1\infty}} \tag{7}$$

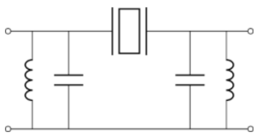

(a) π section: series AWR, shunt pLCR

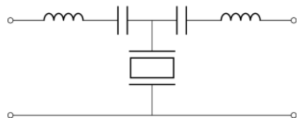

(b) T section: shunt AWR, series sLCR

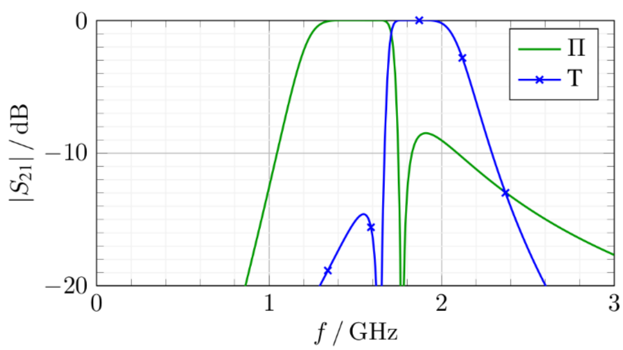

(c) Filter response of a single stage

Fig. 3. Working principle of the two presented complementary filter stages

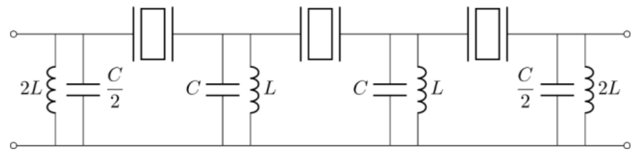

(a) Cascaded π sections: AWR (series), parallel LCR (shunt)

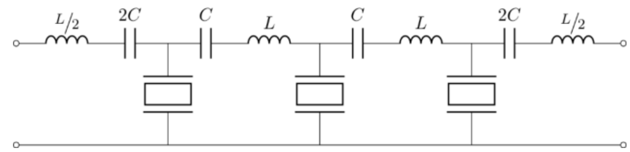

(b) Cascaded T sections: AWR (shunt), series LCR (series)

Fig. 4. Cascaded filter stages (N = 3)

In both equations, the factor q depends on targeted operation bandwidth. From there, it can be seen that there is no theoretical bandwidth limit of the stages. If q is made larger and approaches infinity, this means that for the π-section f_2 approaches $f_{2\infty}$ and for the T-section f_1 approaches $f_{1\infty}$, i.e. in both cases the cut-off frequency approaches the notch frequency. This is no limit in theoretical realizability, in contrast, it means creating a steeper filter skirt.

The typical design of a single stage depends on the realizable capacitance ratio r and the notch placement. These two parameters can be defined in the beginning, i.e. by choosing appropriate AWR material and architecture. It is important to note that the overall bandwidth of the filter stage does not depend on the r and the notch frequency, however, C_0 does. That means that the required resonator area is determined as a result of the filter design procedure. The values of the required lumped inductor and capacitor also depend on targeted filter bandwidth.

B. Cascaded Filter Stages

More advanced filter functionality is based on cascading multiple equally designed stages. By these means, the adjacent LC resonators of the different stages can be combined into single resonators. This is shown in Fig. 4 for cascades of 3 stages.

By doing so, the overall filter behavior is changed, which has significant impact on stopband suppression. As a rough approximation, the overall stopband suppression of N stages can be estimated by N times the stopband suppression of a single stage (see Fig. 5).

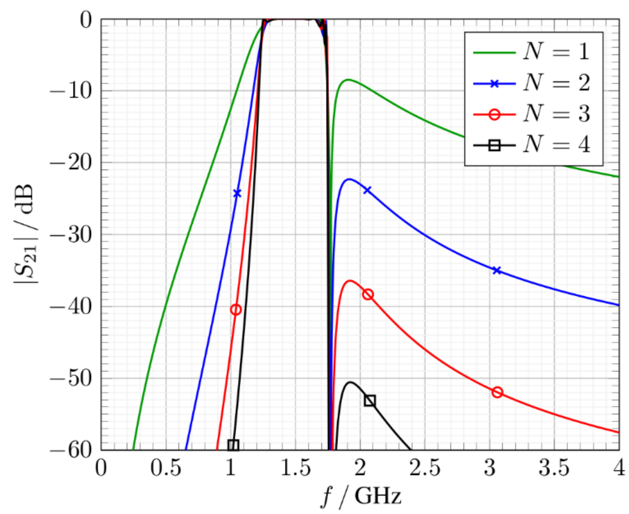

Fig. 5. Filter transmission (calculation) of N cascaded π-type example filter stages (N = 1 to 4)

The typical design process is as follows: First, the resonance frequencies for a suitable acoustic-wave resonator have to be defined. Then, depending on these resonator properties and the desired bandwidth of the filter, the remaining corner frequency is determined by (6) or (7), respectively. The elements of a single stage, including C_0, are then calculated using formulas by Zobel [10]. Afterwards, depending on the required stopband behavior, the number of required stages to be cascaded is determined. Finally, the behavior of the filter can be optimized by tweaking element values and considering finite Q factors.

IV. Application Example

An example filter has been calculated following the procedure outlined above. A resonator with a static capacitance of 1.5 pF was used to give a bandwidth of approximately 500 MHz. A calculation of the filter response of several of the given stages in cascade is shown in Fig. 5. It is observed that the stopband suppression increases significantly with the number of stages, as stated above. The sharp roll-off on the upper side, caused by the resonators, is clearly observable. Furthermore, the higher the number of stages, the higher the roll-off and stopband suppression on the other side of the passband.

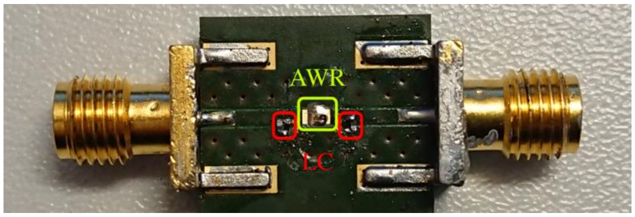

Fig. 6. Photograph of the PCB with mounted components

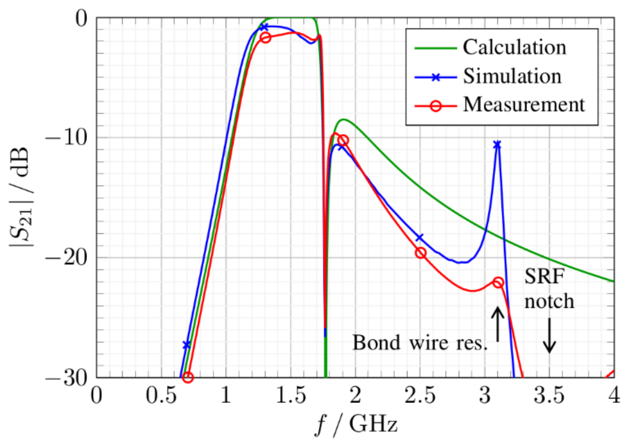

Fig. 7. Filter transmission of a single example filter stage: Comparison of calculation with ideal elements (green), simulation including PCB effects, bond wires, and S-parameter models of elements (blue), and measurement of discrete structure (red)

A test structure for the basic filter stage has been designed, simulated and built on a PCB with discrete components. A photograph of the PCB with the resonator and attached lumped elements is shown in Fig. 6. A comparison of the ideal behavior, a simulation taking EM effects of the PCB, real element models and bond wires into account, and the measurement result are shown in Fig. 7.

The calculation is carried out using the formulas mentioned above. It is already taking into account a slight series resonance shift of the resonator due to the bond wires used for connecting it to the PCB. This is done by assuming a smaller value of r in the design equations. The simulation uses S-parameter files of the employed L and C components, as well as a lumped BVD model for the AWR. It is also taking into account an EM simulation of the PCB and an estimation for the bond wires. The measurement was done with soldered components on the PCB. It fits well to the simulation, but shows a slightly higher insertion loss (IL).

The effect of the bond wires can be seen in the simulation and in the measurement. It results in a parasitic series resonance at 3.1 GHz. Furthermore, an additional notch is observed in simulation and measurement at around 3.5 GHz. This is due to the self-resonance frequency (SRF) of the employed capacitors.

The measurement proves the proposed concept to be feasible for hybrid filter design. It is assumed that an integrated solution can provide lumped elements with higher Q factors and reduce parasitics between the elements. A potential hybrid integration of lumped elements with the acoustic-wave resonator could also reduce required area significantly.

Furthermore, the usage of resonators with the same resonance characteristics is assumed to be suited for wide-band duplexing application with a small transition region between both frequency bands as indicated in Fig. 3c.

V. Conclusion

In this paper, a new filter design concept has been proposed. It is shown that the concept is feasible and how it can be applied to designing arbitrarily-wide-band filters with a sharp roll-off on one side of the passband. The high quality factor of the AWR enables a steep filter skirt without degrading passband performance significantly. Depending on the number of stages, a theoretically unlimited stopband suppression can be achieved. Measurement results of a single stage fit very well to a simulation including bond wire and EM effects of the PCB. Due to equal stages and low component spread, the concept is assumed to be feasible for integration in future technologies. It is, however, important to note that this concept still requires high-Q inductors and capacitors since these elements contribute most to IL. To meet the requirements of a given specification, the resonator impedance must be chosen carefully due to its bandwidth dependency.

References

[1] J.-E. Mueller, T. Bruder, P. Herrero, N. Norholm, P. Olesen, J. Rizk, and L. Schumacher, “Requirements for Reconfigurable 4G Front-Ends,” in *IEEE MTT-S International Microwave Symposium Digest (IMS)*. Seattle, WA: IEEE, Jun. 2013, pp. 1–4.

[2] A. Hagelauer, G. Fattinger, C. C. W. Ruppel, M. Ueda, K. Hashimoto, and A. Tag, “Microwave Acoustic Wave Devices: Recent Advances on Architectures, Modeling, Materials, and Packaging,” *IEEE Transactions on Microwave Theory and Techniques*, pp. 1–15, 2018.

[3] R. Aigner, “SAW and BAW Technologies for RF Filter Applications: A Review of the Relative Strengths and Weaknesses,” in *IEEE Ultrasonics Symposium*. Beijing, China: IEEE, Nov. 2008, pp. 582–589.

[4] R. Aigner, S. Marksteiner, L. Elbrecht, and W. Nessler, “RF-filters in mobile phone applications,” in *12th International Conference on SolidState Sensors, Actuators and Microsystems (TRANSDUCERS)*, vol. 1. Boston, MA, USA: IEEE, Jun. 2003, pp. 891 – 894.

[5] S. Gong and G. Piazza, “Design and Analysis of Lithium-Niobate-Based High Electromechanical Coupling RF-MEMS Resonators for Wideband Filtering,” *IEEE Transactions on Microwave Theory and Techniques*, vol. 61, no. 1, pp. 403–414, Jan. 2013

[6] R. Weigel, D. P. Morgan, J. M. Owens, A. Ballato, K. M. Lakin, K. Hashimoto, and C. C. W. Ruppel, “Microwave Acoustic Materials, Devices, and Applications,” in *IEEE Transactions on Microwave Theory and Techniques*, vol. 50, no. 3. IEEE, Mar. 2002, pp. 738–749.

[7] B. Drafts, “Acoustic Wave Technology Sensors,” *IEEE Transactions on Microwave Theory and Techniques*, vol. 49, no. 4, pp. 795–802, Apr. 2001.

[8] J. D. Larson III, P. D. Bradley, S. Wartenberg, and R. C. Ruby, “Modified Butterworth-Van Dyke Circuit for FBAR Resonators and Automated Measurement System,” in *IEEE Ultrasonics Symposium*, vol. 1. San Juan: IEEE, Oct. 2000, pp. 863–868.

[9] R. Aigner, “Bringing BAW Technology into Volume Production: The Ten Commandments and the Seven Deadly Sins,” in *Third International Symposium on Acoustic Wave Devices for Future Mobile Communication Systems*, Chiba University, 2007.

[10] O. J. Zobel, “Theory and Design of Uniform and Composite Electric Wave-filters,” *The Bell System Technical Journal*, vol. 2, no. 1, pp. 1 – 46, Jan. 1923.